Int. J. Electrochem. Sci., 16 **(2021)** Article ID: 210339, doi: 10.20964/2021.03.37

International Journal of
ELECTROCHEMICAL
SCIENCE
www.electrochemsci.org

Mechanical and Corrosion Properties of 7N01 Aluminum Alloy After Non-isothermal Heat Treatment under Different Quenching Conditions

Shuai Li[1,2,*], *Zhongying Liu*[2], *Feng Mao*[1], *Xingxing Wang*[2,*], *Xiaogang Hu*[3], *Lei Shi*[4], *Honggang Dong*[4], *Linjian Shangguan*[2*]

[1] National Joint Engineering Research Center for Abrasion Control and Molding of Metal Materials, Henan University of Science & Technology, Luoyang, 471003, PR China
[2] School of Mechanical Engineering, North China University of Water Resources and Electric Power, Zhengzhou 450045, PR China
[3] XI' AN Rare Metal materials Institute Co.Ltd, Xi'an 710016, PR China
[4] School of Materials Science and Engineering, Dalian University of Technology, Dalian 116024, PR China
[*]E-mail: lyctlishuai@163.com (Shuai Li); paperwxx@126.com (Xingxing Wang); sgljbh@163.com (Linjian Shangguan)

Received: 23 October 2020 / *Accepted:* 16 December 2020 / *Published:* 31 January 2021

The mechanical properties and corrosion susceptibility of the welded 7N01 aluminum alloy change after the mandatory heat straightening due to the post-welded thermal cycles. It can cause severe safety issues for the structural parts. Herein, we used non-isothermal heat treatment to simulate a heat straightening process and investigated the effect of quenching conditions on the microstructure and properties of 7N01 aluminum alloy. The non-isothermal heat treatment deteriorates the corrosion resistance and mechanical properties of 7N01 aluminum alloy, due to the formation of GP zones during natural aging. Since the cooling rate results in the difference in potential between the matrix and the grain boundary precipitates in 7N01 aluminum alloy, the corrosion resistance of heat-treated samples ranks in the following order: base metal >water quenched >oil quenched > air quenched.

Keywords: Heat straightening; 7N01 aluminum alloy; non-isothermal heat treatment; corrosion susceptibility

1. INTRODUCTION

Welding is widely applied in the manufacturing industry and the control of distortion is a challenge in the welding process[1, 2]. It will affect the assembly accuracy, results in a substantial deterioration in the properties (strength and corrosion resistance, etc.) of structural parts[1, 2]. The welding distortion is inevitable due to the heterogeneous thermal cycles during the welding process.

Especially, the 7N01 aluminum alloy, which has low yield strength and high linear thermal expansion coefficient, is prone to induce distortion during the welding process [3, 4]. Consequently, heat straightening is always performed to regulate the welding distortion in the manufacturing of 7N01 aluminum alloy structural parts[5, 6]. However, the extra thermal cycles easily cause new problems to the reliability of welded joints [5, 6]. The heat straightening is a non-isothermal heat treatment. At present, many investigations have been performed to reveal the evolution of mechanical and corrosion properties during heat straightening [4-8]. The evolution of mechanical properties after the different numbers of times in heat straightening was studied using oxy-acetylene flame, and pointed out that the mechanical properties showed different change trends at different flame correction temperatures [8]. The effect of heat straightening on the corrosion susceptibility was investigated using heat treatment, and found out that the corrosion resistance reduced with increasing the number of times of heat straightening [5, 9]. The properties of 7N01 aluminum alloys after heat straightening is associated with the peak temperature, heating speed and cooling rate. The supersaturated solid solution forms during the heating process, then it displays different quenching sensitivity based on the various quenching conditions. The relevant researches showed that the quenching condition has an important effect on the microstructure and properties of age strengthening aluminum alloys[10, 11]. Therefore, the quenching sensitivity of age strengthening aluminum alloys has attracted great attention from industry and academia. And the cooling rate is one of the extremely important parameters in the heat treatment process. In this paper, the non-isothermal heat treatment experiment is performed to simulate the heat straightening. And the quenching sensitivity of 7N01 aluminum alloy after non-isothermals with different quenching media (water, oil and air air at room temperature) is investigated. The aim is to study the effect of quenching sensitivity during heat straightening.

2. EXPERIMENTAL PROCEDURE

2.1 Non-isothermal heat treatment

The heat treatment specimens with the sizes of 40 mm ×150 mm × 5 mm were obtained from the 7N01 aluminum alloy with T4 condition and the chemical composition of the alloy is listed in Table 1. During heat treatment, the 7N01 aluminum alloy samples were heated to the peak temperature of 300 ^{o}C, and then immediately quenched in water, oil or air at room temperature. Then the specimens were taken out when the specimens were cooled to room temperature. The schematic diagram of non-isothermal heat treatment of the simulation of heat straightening is shown in Fig.1. The duration of the heating stage is around 95 s and the quenching time is controlled within 3 s. The water quenching has the largest cooling rate, which can cool the alloy to room temperature instantaneously. The cooling rate in oil is lower than that in water and the corresponding quenching process can be divided into two stages. First, the temperature of heat-treated samples decreased from the peak temperature to a lower temperature (about 100 ^{o}C) immediately, and then cooled to room temperature at a slower rate. The air quenching samples have a similar temperature trend with the oil quenching specimens. However, the cooling rate is lower than that in oil and the cooling process lasts for about 40 min.

Table 1. Chemical composition of 7N01-T4 aluminum alloy (wt. %)

Element	Mg	Zn	Cu	Mn	Fe	Cr	Si	Ti	Zr	V	Al
Contents	4.76	1.20	0.01	0.42	0.11	0.11	0.04	0.04	0.07	0.01	Bal.

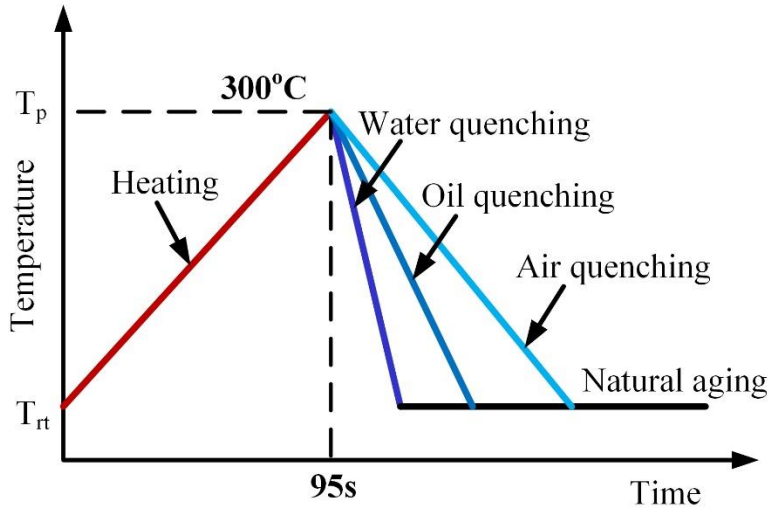

Figure 1. Schematic diagram of non-isothermal heat treatment

2.2 Immersion corrosion and electrochemical tests

The intergranular corrosion tests were carried out according to the standard of G110-92[12]. The testing specimens were prepared with a dimension of 40 mm × 25 mm × 5mm. The immersion corrosion time is 12 h with the temperature of 35 ºC. The exfoliation corrosion experiments were performed based on the standard of G34-01[13]. The exfoliation corrosion specimens were obtained with the sizes of 40 mm × 30 mm ×5 mm and the experimental temperature was set as 25 ºC. The evolution of corrosion morphology during the exfoliation corrosion test was recorded at different immersion time. All the immersion corrosion experiments were performed for three times.

The electrochemical tests were carried out by using the CS350 electrochemical workstation. A typical three-electrode system was used to conduct the potentiodynamic polarization test. The reference electrode and counter electrode are Ag/AgCl (saturation KCl) and large platinum sheet, respectively and the investigated 7N01 aluminum alloy as the working electrode. The electrochemical experiments were conducted in 1 M NaCl solution with the scan rate of 1mV/s and the testing range is ±0.2 V (relative to the open circuit potential). The potentiodynamic polarization experiments were carried out after the open circuit potential to keep the potential stable and the exposed area of the electrochemical testing samples was 0.95 cm^2.

2.3 Mechanical property test and microstructure investigation

The sizes of the tensile test specimens are illustrated in Fig. 2 and the mechanical property

experiment was conducted on DNS100 type apparatus (Changchun Testing Machine Institute Co., LTD) with the tensile speed of 5 mm/min. The micro-hardness test was carried out on MVC-1000B type Vickers micro-hardness tester according to GB/T4340.1-2009 standard. The load is 0.1 N with the duration time of 15 s. All the micro-hardness values were tested five times to ensure accuracy.

The intergranular corrosion depth was observed on Leica MEF4 Optical Microscope (OM). And the fracture morphology of tensile specimens and corrosion features of electrochemical experiments were conducted on Zeiss Supra55 Scanning Electron Microscope (SEM) apparatus. To analyze the reason for the evolution of mechanical properties and corrosion susceptibility of 7N01 aluminum alloys, the Transmission Electron Microscope (TEM) tests were performed on a Tecnai G^2 20 S-Twin (FEI Co.) device. The TEM samples were prepared by twin-jet electropolishing and the mixture solution is HNO_3: ethanol = 1:4, which is cooled to -25 ^oC. The Differential Scanning Calorimetry (DSC) tests were performed to discuss the evolution of precipitates of 7N01 aluminum alloy. The weight of the DSC sample is around 20 mg. During the experiment, the samples were heated from room temperature to 450 ^oC with a heating rate of 10 ^oC/min.

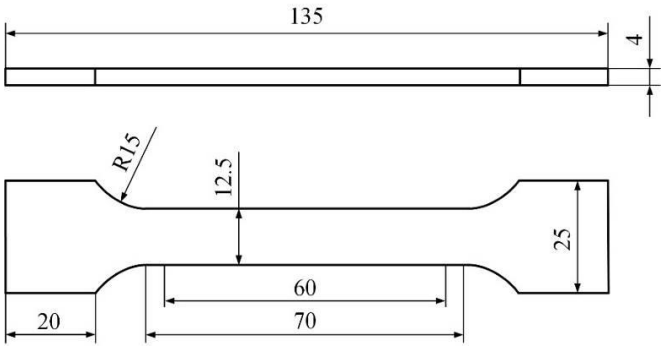

Figure 2. Dimensions of the specimens for the tensile test (mm)

3. RESULTS

3.1 Mechanic Property

Figure 3 shows the micro-hardness of 7N01 aluminum alloy after quenching. The natural aging effect occurred for the 7N01 aluminum alloy after non-isothermal heat treatment. The evolution of micro-hardness can be divided into two stages: first fast-rising stage and then it tends to stable values. The stable values of micro-hardness rank in the following order: water quenching > oil quenching > air quenching. This phenomenon shows that the three quenching mediums have a different effect on the evolution of properties of 7N01 aluminum alloy. It is emphasized that all the experiments of specimens were carried out 45 days later after heat treatment considering the natural aging effect.

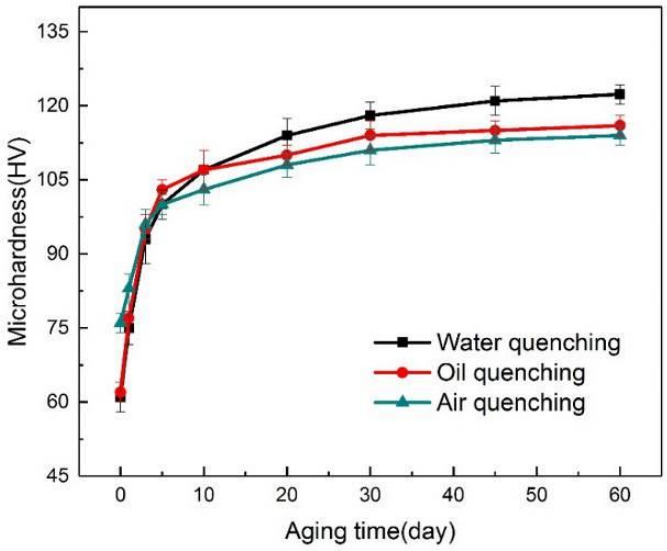

Figure 3. Evolution of micro-hardness during room temperature aging after non-isothermal heat treatment under different quenching conditions

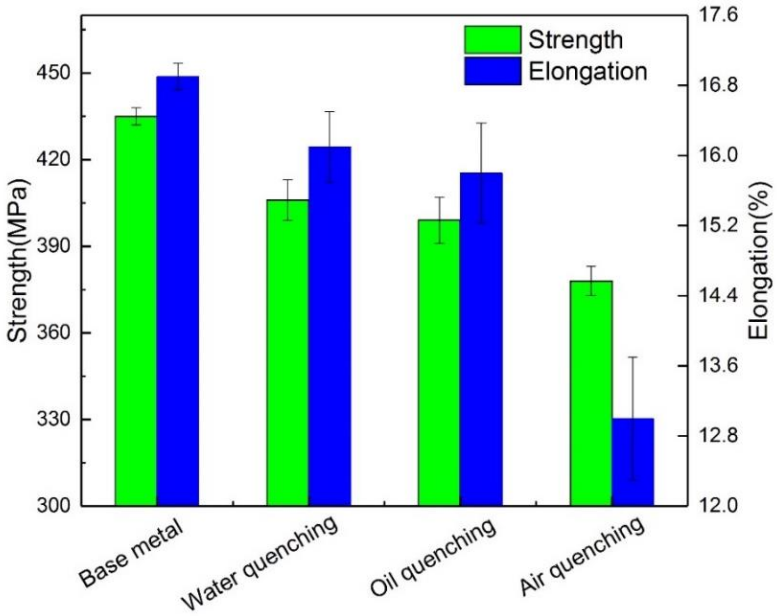

Figure 4. The tensile strength and elongation of 7N01 aluminum alloys under different quenching conditions

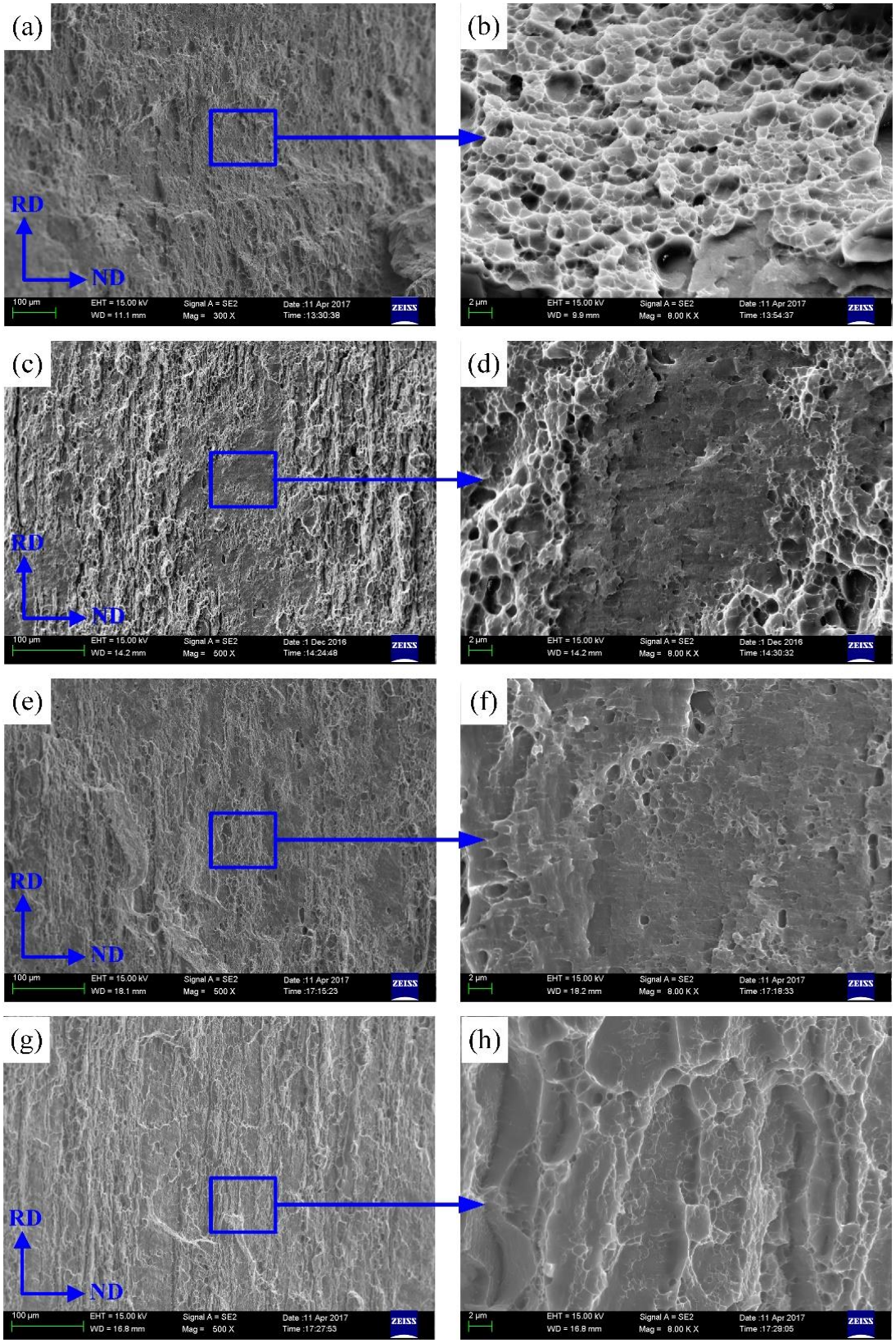

Figure 5. SEM images of the fracture morphology of (a)-(b) base metal and samples after non-isothermal heat treatment for (c)-(d) water quenching, (e)-(f) oil quenching, (g)-(h) air quenching

The change of mechanical properties of 7N01 aluminum alloy under different quenching conditions is illustrated in Fig.4. The non-isothermal heat treatment deteriorates the mechanical properties of the 7N01 aluminum alloy. The mechanical properties decreased with the reduction of the cooling rate during quenching. Necking phenomenon occurred near the fracture of the tensile testing specimens after non-isothermal heat treatment under different quenching conditions. The fracture morphology of base metal displays ductile features with uniform dimples as shown in Fig.5 a-b. The specimens of water and oil quenching have similar fracture characteristics, which are dominated by cleavage planes and fine dimples, as displayed in Fig.5c-f. For the fracture morphology of the air quenching sample, layer-like fracture features appear at low magnification (in Fig.5g). Lots of fine dimples appear in high magnification, which is caused by the intercrystalline micropore aggregation, as displayed in Fig.5 h. This phenomenon may be related to the plastic deformation of the precipitate-free zone near the grain boundary when fractured [14, 15].

3.2 Corrosion behavior

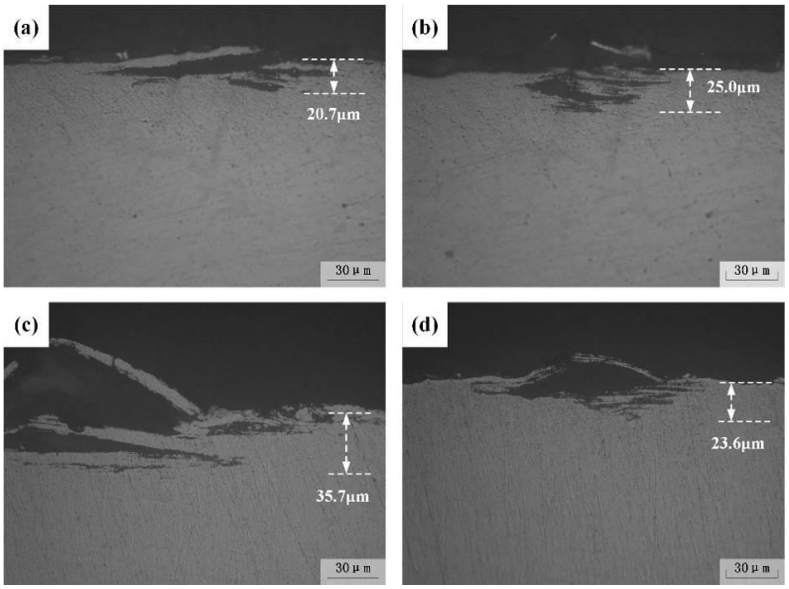

Figure 6. Intergranular corrosion morphology in (a) 7N01 aluminum alloy base metal and samples after non-isothermal heat treatment at 300 ^{o}C for (b) water quenching, (c) oil quenching, and (d) air quenching

The morphology of intergranular corrosion of 7N01 aluminum alloy after non-isothermal heat treatment under different quenching conditions is shown in Fig. 6. The corrosion resistance of 7N01 aluminum alloy deteriorates after non-isothermal heat treatment. And the corrosion depth of sample quenching in oil is around 35.7 μm, which shows higher corrosion susceptibility than those of the samples quenching in other media. The maximum intergranular corrosion depth of the sample quenching in the air is about 23.6 μm, which is between the base metal and the water quenching samples. The intergranular corrosion morphology of oil and air quenching samples are dominated by pitting and exfoliation corrosion. There is no typical network-like intergranular corrosion morphology. These characteristics are similar to those of base metal and water-quenched samples.

The exfoliation corrosion morphology of 7N01 aluminum alloy after non-isothermal heat treatment under different quenching conditions is shown in Fig. 6. The phenomenon of exfoliation corrosion of oil and air quenching samples appears after immersion in the corrosive solution for 6 h, which shows higher exfoliation corrosion susceptibility than those of base metal and water quenching samples. The surface layers on the oil and air quenching samples have fallen off after immersion in the corrosive solution for 12 h and the degree of exfoliation corrosion is significantly greater than those of the base metal and the water quenching sample. The exfoliation corrosion morphology of samples under different quenching conditions has no significant change when the immersion time is more than 12 h.

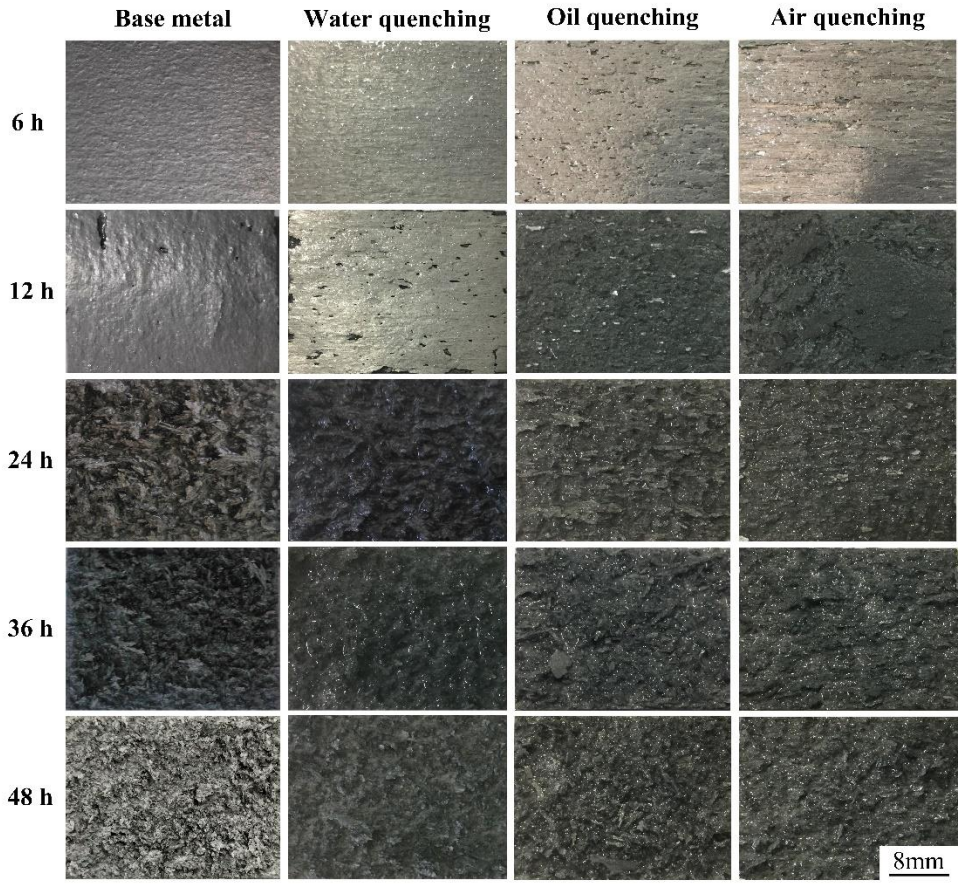

Figure 7. Exfoliation corrosion morphology for 7N01 aluminum alloy under different conditions

3.3 Electrochemical properties

Fig. 8 shows the change of the open circuit potential of 7N01 aluminum alloy after the non-isothermal heat treatment under different quenching conditions. The values of the the open circuit potential of samples have reached a stable state and slightly fluctuated near the stable value after testing for 30 min. The evolution of the open circuit potential of the heat treatment specimens is mainly related to the change of grain boundary precipitates, which is caused by the thermal cycles during different quenching conditions[16]. The dynamic potential polarization curve of samples is shown in Fig.9. The

polarization curves of samples under different quenching conditions are similar. As the over-potential of the anode increases, the polarization current density of samples increases and then gradually approaches a certain stable value. The fitting results of polarization curves of samples under different quenching conditions are listed in Table 2. The self-corrosion potential of the oil quenching sample is lower than those of the air quenching sample and the base metal, and higher than that of the water quenching sample. In terms of corrosion current density, the value of oil quenching sample is the largest, followed by the air quenching sample, which is higher significantly than those of the base metal and water quenching sample. The corrosion rate has a similar evolution trend. The corrosion resistance of 7N01 aluminum alloys deteriorates significantly after non-isothermal heat treatment with oil and air quenching conditions based on the results of polarization curves.

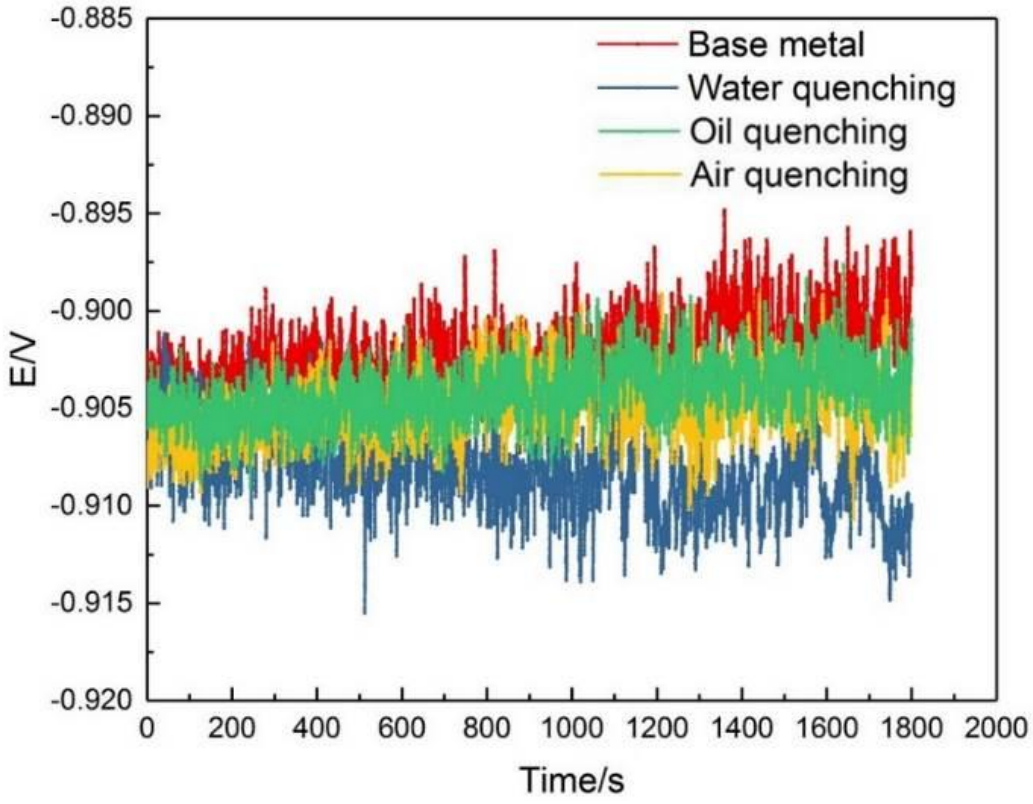

Figure 8. Open circuit potential of 7N01 aluminum alloy in 1M NaCl aqueous solution under different quenching conditions

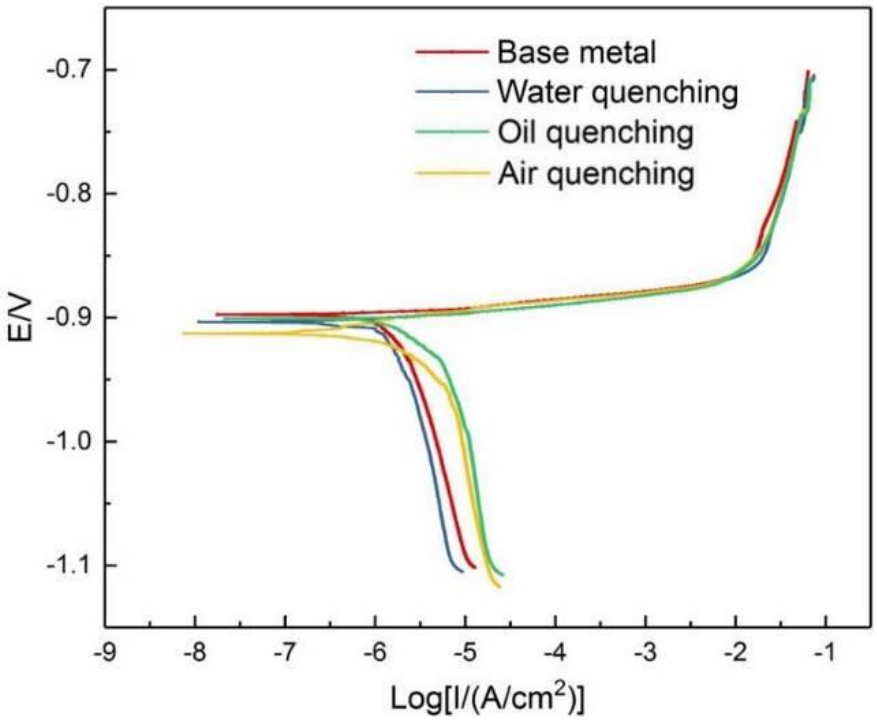

Figure 9. Potential dynamic polarization curves of 7N01 aluminum alloy in 1M NaCl aqueous solution under different quenching conditions

Table 2. Electrochemistry corrosion parameters of 7N01 aluminum alloy in 1M NaCl aqueous solution under different quenching conditions

Condition	Corrosion potential (V)	Corrosion current density (mA/cm^2)	Corrosion rate (mm/a)
Base metal	-0.899	2.150×10^{-6}	0.07306
Water quenching	-0.906	1.933×10^{-6}	0.06568
Oil quenching	-0.890	6.086×10^{-6}	0.20679
Air quenching	-0.895	5.088×10^{-6}	0.17288

3.4 Microstructure evolution

The distribution of precipitates in the matrix of non-isothermal heat treatment samples under different quenching conditions is shown in Fig.10. It can be seen that the morphology of precipitates in the matrix is different, which is attributed to the different quenching conditions, as shown in Fig.10a-d. There are no obvious precipitates in the matrix of base metal and water quenching sample, as shown in Fig.10a-b. While disc-like and rod-like precipitates are formed in the oil and air quenching samples. The relevant investigations have proved that the precipitates are mainly η phases, which are formed during the quenching process. Additionally, there are a large number of high density and fine GP zones in the matrix of the heat-treated specimens, which attributed to the natural aging of 7N01 aluminum alloy, as shown in Fig.10 a1 and Fig.10 b1.

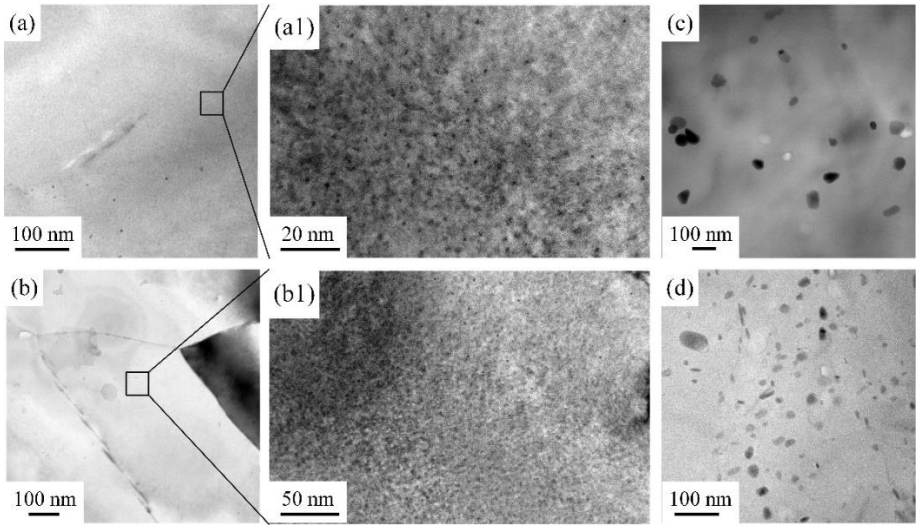

Figure 10. TEM images of matrix morphology in 7N01 aluminum alloy for (a) base metal,(a1) the magnified image of (a), (b) water quenching, (b1) the magnified image of (b),(c) oil quenching and (d) air quenching

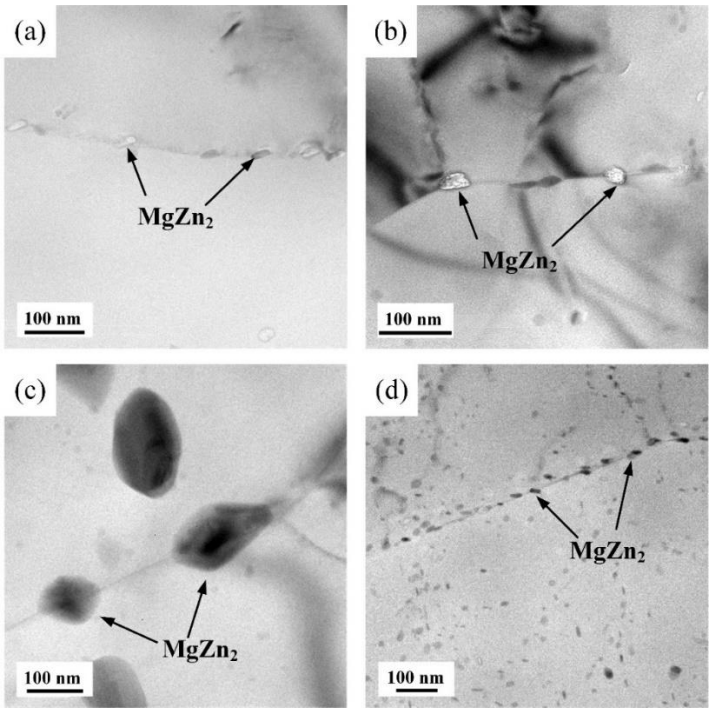

Figure 11. TEM images of grain boundary morphology in 7N01 aluminum alloy for (a) base metal and samples after non-isothermal heat treatment at a peak temperature of 300°C for (b) water quenching, (c) oil quenching, and (d) air quenching

The TEM images of grain boundary precipitates of non-isothermal heat treatment samples under different quenching conditions are shown in Fig.11. The size of the precipitates at the grain boundary of the oil-quenched sample is larger than those of another specimen. The size of precipitates at the grain boundary of the air quenching sample decreased slightly, while the density and quantity of precipitates

increased. Many precipitates in the matrix form on both sides of grain boundaries. It should be noted that the precipitate-free zone is not observed near the grain boundary for all the samples.

4. DISCUSSION

The evolution of mechanical properties and corrosion susceptibility are mainly associated with the change of precipitates of Al-Zn-Mg(Cu) alloy[17-19]. And the evolution of the precipitates in 7N01 aluminum alloy is related to the thermal cycles[17-19]. Consequently, it is necessary to analyze the thermal cycles of heat-treated samples before discussing the evolution mechanism of mechanical properties and corrosion susceptibility. For the heat-treated specimens, the thermal cycles can be divided into three stages: heating process, quenching process, and natural aging. All heat-treated specimens have the same heating process and natural aging. As a result, the differences in mechanical properties and corrosion susceptibility are caused by different quenching process. The investigations have proved that the critical cooling rate of the η phase is around 100 ^{o}C/s[20, 21]. For oil and air quenching samples, the cooling rate during the quenching process is lower than 100 ^{o}C/s. Therefore, disc-like and rod-like precipitates form, as shown in Fig.10. For the water quenching sample, η phases do not form because the cooling rate during water quenching is higher than 100 ^{o}C/s. The formation of η phase results in the decrease of solute elements in the matrix then the natural aging effect reduced, namely the quantity of GP zones decrease. It is reported that a peak strength of Al-Zn-Mg(Cu) can be achieved when the matrix precipitates are mainly dominated by the GP zones[22]. Consequently, the mechanical properties of the heat-treated sample rank in the following order: base metal >water quenching > oil quenching > air quenching, as shown in Fig.3-4. The corrosion susceptibility of Al-Zn-Mg(Cu) is mainly associated with the potential difference between the grain boundary precipitates and the matrix[4, 16]. It is well known that the longer duration of quenching process means the longer time of diffusion of solute elements. Then the potential difference between the grain boundary precipitates and the matrix will change, which will result in the evolution of corrosion susceptibility of 7N01 aluminum alloy. For the heat-treated samples, the air quenching specimen suffered the longer duration of the quenching process compare to those of another samples, and the potential difference between the matrix and grain boundary precipitates increase significantly. Consequently, the corrosion resistance of the heat-treated sample ranks in the following order: base metal >water quenching > oil quenching > air quenching.

5. CONCLUSION

The non-isothermal heat treatment deteriorates the mechanical properties and corrosion resistance of 7N01 aluminum alloy. The natural aging has a significant effect on the mechanical properties of 7N01 aluminum alloy, which is attributed to the formation of GP zones. The cooling rate affects the evolution of the potential difference between the matrix and grain boundary precipitates of 7N01 aluminum alloy, and then the corrosion resistance of heat-treated sample ranks in the following order: base metal >water quenching >oil quenching > air quenching.

ACKNOWLEDGMENTS
This research was funded by Natural Science Foundation Youth Science Fund Project and Excellent Youth Project of Henan (Nos. 202300410272 and 202300410268), the China Ministry of Education's industry-academy cooperation in collaboration with the education project (201901078004 and 201901078022), Open Fund of National Joint Engineering Research Center for Abrasion Control and Molding of Metal Materials (No. HKDNM2019020), the National Natural Science Foundation of China (51705151 and 52071165), the China Postdoctoral Science Foundation (2019M662011), Open Fund of State Key Laboratory of Advanced Brazing Filler Metals and Technology (SKLABFMT201901), Open Fund of State Key Laboratory of Advanced Welding and Joining (AWJ-21M11), and Key Technology Needs of Henan Province Unveiled and Solved Project (191110111000).

References

1. D. Deng, *Mater. Design.*, 30 (2009) 359.
2. D. Deng and H. Murakawa, *Comp. mater. Sci.*, 43 (2008) 353.
3. S. Li, H. Dong, L. Shi, P. Li and F. Ye, *Corros. Sci.*, 123 (2017) 243.
4. S. Li, H. Dong, P. Li and S Chen, *Corros. Sci.*, 13 (2018) 278.
5. S. Li, D. Guo and H.G.Dong, *T.Nonferr. Metal. Soc.*, 27 (2017) 250.
6. S. Li, H.G. Dong, X.X.Wang, Z. Liu, L.J. Shangguan and S.Y. Tian, *Materials*., 12 (2019) 2949.
7. X. M. Wang, B. Li, M.X Li, C. Huang and H. Chen, *Mat. Sci. Eng. A*, 688 (2017) 114.
8. H. Lu, L. Shi, H. Dong, S.Li, D.Guo and C.Tao, *J. Alloy. Compd.*, 689 (2016) 278.
9. H. Dong, Y.Wang, L. Shi, P. Li and S. Li, Mater. Res. Express, 6 (2019) 9650.
10. S.D. Liu, B. Chen, C.B. Li, Y. Dai, Y.L. Deng and X.M. Zhang. *Corros. Sci.*, 91 (2015) 203.
11. I.Westermann, A.L.Haugstad, Y. Langsrud and K. Marthinsen, *T.Nonferr. Metal. Soc.*, 22 (2012)1872.
12. ASTM G110-92. Standard Practice for Evaluating Intergranular Corrosion Resistance of Heat Treatable Aluminum Alloys by Immersion in Sodium Chloride + Hydrogen Peroxide Solution; *American Society for Testing Materials*, ASTM: West Conshohocken, PA, USA, 2009.
13. G34-01. Standard Test Method for Exfoliation Corrosion Susceptibility in 2xxx and 7xxx Series Aluminum Alloys (EXCO Test); *American Society for Testing Materials*, ASTM: West Conshohocken, PA, USA, 2013
14. D. Wang and Z.Y. Ma, *J. Alloy. Compd.*, 469 (2009) 445.
15. D.Wang and Z.Y. Ma, Z. M. Gao, *Mater. Chem. Phys.*, 117 (2009) 228.
16. F. Song, X. Zhang, S. Liu, Q.Tan and D. Li, *Corros. Sci.*, *78* (2014) 276.
17. Y. Liu, S.Liang and D. Jiang, *J. Alloy. Compd.*, 689 (2016) 632.
18. M. Kumar and N.G. Ross, *J. Mater. Process. Tech.*, 231(2016) 189.
19. P.K. Rout, M.M. Ghosh and K.S. Ghosh, *Mater. Charact.*, 104 (2015) 49.
20. B.Yang, B.Milkereit, Y. Zhang, P.A.Rometsch, O. Kessler and C. Schick, *Mater. Charact.*, 120 (2016) 30.
21. D. Zohrabyan, B. Milkereit, C.Schick and O. Kessler, *T.Nonferr. Metal. Soc.*, 24 (2014) 2018.
22. J.T. Staley, *Mater. Trans.*, 5 (1974) 929.